Tree-like alumina nanopores generated in a non-steady-state anodization†

Wenlong Cheng,‡*[a] Martin Steinhart,[a] Ulrich Gösele[a] and Ralf B. Wehrspohn[b]

Received 25th June 2007, Accepted 24th July 2007
First published as an Advance Article on the web 30th July 2007
DOI: 10.1039/b709618f

Novel tree-like alumina nanopores were reproducibly obtained in non-steady-state anodization conditions by exponential decrease of anodization potential. The mechanism of pore formation was thought to be due to a combination of electrical treeing and mechanic stress in the growth process. Furthermore, some interesting properties from gold nanotrees were observed showing that the tree-like nanopores will be new templates towards fabrication of nanotrees from a variety of materials possibly exhibiting new shape-dependent properties.

Nanoporous alumina formed by electrochemical anodization of aluminium in acid electrolytes has been extensively studied for more than 50 years.[1] Wood's model[2] and further modified models[3,4] can give satisfactory interpretations of many experimental phenomena, such as monodispersity of pore size distribution, linear dependence of pore diameter and inter-pore distance on the applied anodization potential. However, these models cannot easily explain well some recent findings, such as self-ordered pore growth in two-step anodization,[5,6] self-ordering under high-field anodization[7,8] and at burning potential,[9] guided pore growth by imprint lithography,[10,11] *etc.* In order to understand the self-ordering pore growth mechanism, repulsive interactions between the pores[12] and high electric field theory[7–9] have been proposed. In contrast to the extensive research efforts on steady-state anodization, non-steady-state anodization has been given little attention. Here, it was found that unexpected tree-like alumina nanopores were generated in non-steady-state anodization when the anodization potential was decreased exponentially in a stepwise way. The development of pores is more like that of tree or root in nature, which cannot be simply explained by Wood's models.[2–4] Due to its similarity to electrical treeing in insulative materials under voltage aging,[13–16] it is thought that partial discharge (PD) could occur as a result of continuous charge buildup in non-steady-state anodization conditions. In addition, some preliminary results of gold nanotrees indicate that the tree-like nanopores provide the materials science community with a new template towards fabrication of various types of tree-like nanostructures (metal, semiconductor, carbon, polymer) because the template approach has no limitation to material types, and it could find applications in plasmonic waveguiding devices, nonlinear optics, and hierarchical materials assembly, *etc.*[17,18]

Scheme 1 illustrates the fabrication process of tree-like alumina nanopores. Firstly, ordered nanopore arrays were fabricated *via* well-established two-step anodization in oxalic acid at 40 V (see details in ESI†). The nanopores have a depth of ~2 μm, and a diameter of ~35 nm. Then, the anodization potential was decreased exponentially from 40 V to 5 V. The change of the applied anodization potential as a function of time is shown in Fig. 1A. The recorded current–time curve is shown in Fig. 1B. Note that the anodic current decreased immediately upon potential decrease and then increased as a function of time. When a second potential step was applied, the same electrical behavior was repeated. Such behavior repeated until the final potential decreased to 5 V. Thus, a toothed current curve was obtained. It is known that the barrier layer thickness is constant in steady-state anodizations condition because the formation rate at the alumina/oxide interface and the dissolution rate of oxide at the oxide/electrolyte interface are equal.[2,19] When the anodization potential is lowered, the oxide formation rate will decrease as a result of reduced numbers of electrogenerated Al^{3+} ions; however

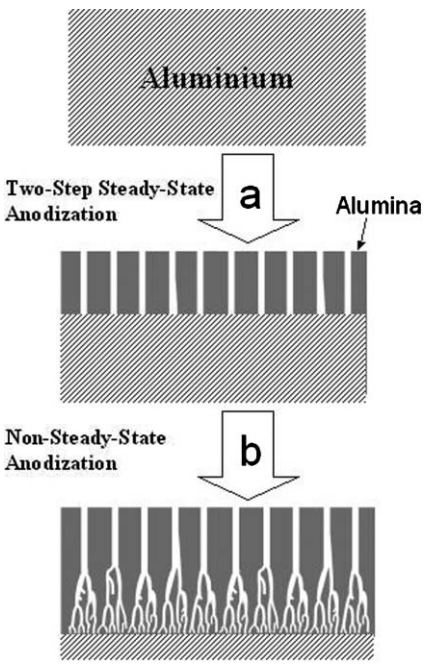

Scheme 1 Schematic diagram illustrating the fabrication process of tree-like alumina nanopores.

[a]*Max Planck Institute of Microstructure Physics, Weinberg 2, D-06120, Halle, Germany*
[b]*University of Paderborn, Department of Physics, Warburger Str. 100, 33098, Paderborn, Germany*
† Electronic supplementary information (ESI) available: Experimental details. See DOI: 10.1039/b709618f
‡ Present Address: Department of Biological and Environmental Engineering, Cornell University, 149 Riley-Robb Hall, Ithaca, NY 14853, USA. Email: wc272@cornell.edu; Fax: +1 607-255-4080; Tel: +1 607-255-6223.

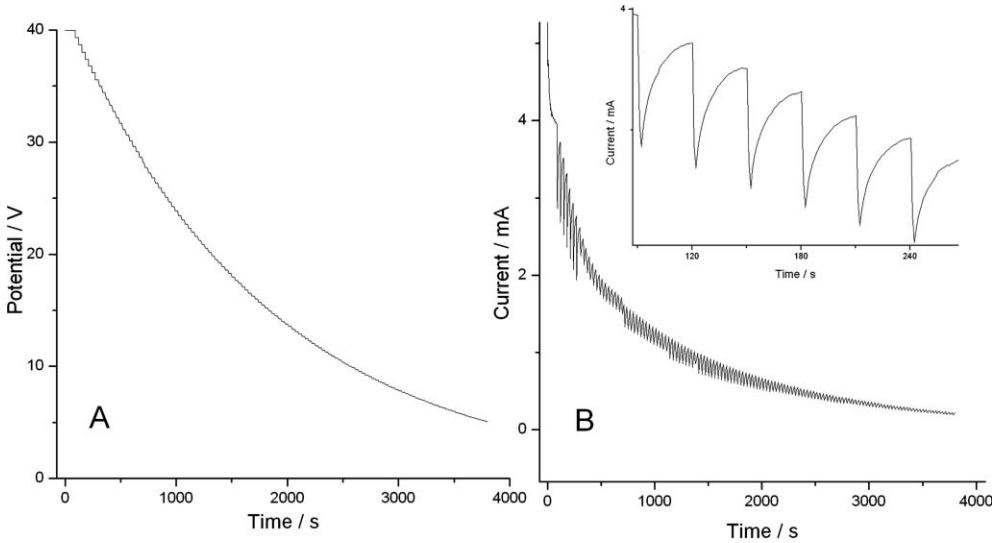

Fig. 1 (A) Potential–time and (B) current–time curves recorded in non-steady-state anodization. Inset of B is a magnified view of the partial current curve.

the local chemical microenvironments at the bottom of the pores are unchanged, therefore, the rate of oxide dissolution is greater than the formation rate, and the net effect is that the barrier layer begins to dissolve. As a result, the barrier layer will begin to thin, which will result in an increase of anodic current. The increasing anodic current is beneficial to the formation rate of the oxide layer due to increasing Al^{3+} ions generated. Thus, a balance of the oxide formation and dissolution will tend to build up again, showing that the anodization process is highly self-adjustable. Before a balance was built up, a second potential reduction was exerted to repeat the same non-steady-state anodization process. When potential reduction steps were applied stepwise, the currents decreased in a toothed shape. Therefore, the whole anodization process was kept in a non-steady state.

The pore morphologies in the non-steady anodization are not predictable based on the currently available models. It is interesting to note that continuous non-steady-state anodization, in fact, resulted in the generation of tree-like nanopores. To improve contrast in cross-sectional analysis of the porous alumina films, the pores were copied with gold replicas using a pulsed electrodeposition method (see ESI†). Fig. 2 shows a TEM micrograph of a microtomed specimen of gold impregnated alumina membrane, showing the highly branched gold nanostructures obtained. The micrographs of two released individual gold nanotrees are shown in Fig. 3A and B, demonstrating that tree-like gold nanostructures are straightforward. It has to be noted that the pore structure is different from Li's and Meng's reports,[20,21] where branched nanopores were obtained in steady-state conditions based on the rationale that the pore diameter is proportional to the applied potential.[2,19] Compared with the pore morphologies obtained in steady-state conditions, several unusual characteristics have to be noted for the non-steady-state conditions: (1) the pore growth direction deviates from the perpendicular axis to the substrate (*e.g.* position 1 in Fig. 3A), some pores can even suddenly change their growth direction at a certain point (*e.g.* position 2 in Fig. 3B); (2) the individual pore develops unevenly, there exist some nodes in each individual pore branch (*e.g.* position 3 in Fig. 3B); (3) once a certain pore ramifies, it grows into only two branched pores (*e.g.* position 4 in Fig. 3B).

These morphological characteristics cannot be simply interpreted by Wood's model which addressed field distribution at the pore bottom in steady-state anodization conditions. It seems that

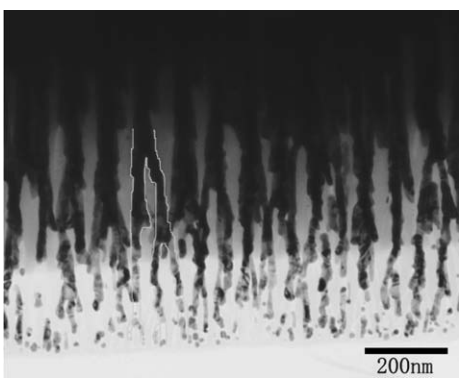

Fig. 2 TEM micrograph of cross-sectional microtomed gold impregnated nanoporous alumina film.

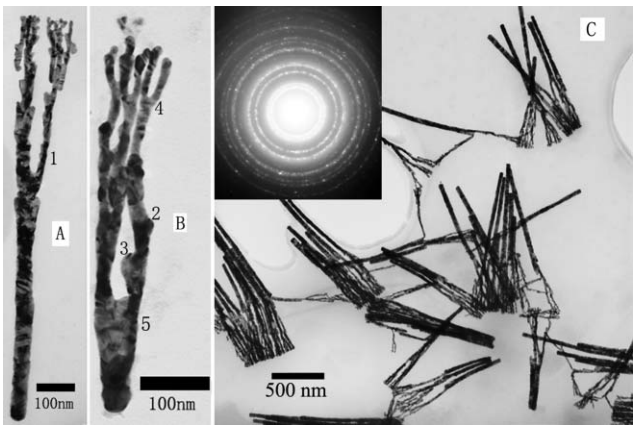

Fig. 3 TEM micrographs of the released gold nanotrees.

the non-steady-state pore growth process here is more like the development of a tree or root in nature, which is reminiscent of electrical treeing in insulative materials under voltage aging.[13–16] Under our experimental conditions, negative charges (from oxygen-containing species, OH^- and O^{2-}) will build up in the oxide layer due to the unbalanced formation and dissolution rates of oxide. The negative charges will accumulate in continuous non-steady-state anodization conditions. At a certain threshold, partial discharges (PD) might take place leading to non-uniform branched current pathways in the oxide layer. Thus, field-induced dissolution[8,12] would result in the generation of branched pores. In addition to the electrical treeing effect, it seems that mechanical stress[12] also played a role in regulating pore morphology. When a new pore wants to develop from its father pores, it has to overcome repulsion forces from its neighboring pores. If the pore succeeds in growing, the father pore will branch into two pores; if it fails, it will end up with a node. The strong pore contests in space make the growth direction deviate from the perpendicular axis and make it impossible for a certain pore to develop into more than two pores. In addition, it also has to be noted that the junction of the father pore and its branched pores often has a larger diameter than father pore itself (*e.g.* position 5 in Fig. 3B). This can be interpreted by the dissolution of the barrier layer as a result of decreasing oxide formation rate at the moment the voltage was decreased, which is consistent with the electrical behavior in Fig. 1B. It also indicates that the pore diameter is not proportional to the anodization potential although it holds true in the steady-state anodization conditions.[2]

It is expected that the as-obtained tree-like nanopores will be a new type of template for tree-like nanostructures possibly exhibiting novel size- and shape-dependent optical, electrical, magnetic, and mechanical properties,[17,18] which can be fabricated *via* electrodeposition[5,22–26] or direct electroless infiltration.[27–30] As an example, some preliminary studies on gold nanotrees are described here. The pulsed electrodeposition resulted in rather uniform infiltration of gold into tree-like nanopores (see S1, S2 in ESI†). The electron diffraction pattern of released gold nanotrees shows a highly crystalline nature as shown in the inset of Fig. 3C. When aluminium was selectively removed by a solution containing 6.8 g copper(II) chloride dihydrate ($CuCl_2 \cdot 2H_2O$), 200 ml 37% HCl and 200 ml deionised water, ordered gold nanotree arrays in a transparent alumina membrane were obtained. We observed that the stem side of the gold nanotree arrays shows a dark red color, the branch side shows a golden reflection. The color duality may originate from the gradient structure of the gold nanotree film, which can be explained by the surface plasmon resonance band from nanogold. The gold stems are well separated from each other, and plasmon coupling does not occur so that a red color was exhibited; the nanogold branches are close to each other so that strong plasmon coupling occurs to result in bulk-gold-like reflection. Further quantitative optical investigations and modeling on these ordered plasmonic nanotree arrays will be undertaken later. Another interesting finding of the gold nanotrees is that the interactions among the gold branches seem to be stronger than those among the gold stems, therefore, the gold nanotrees tended to aggregate *via* their branched parts (Fig. 3C, S3 in ESI†). This might result from the high surface energy of the branched parts due to their high surface-to-volume ratio. The favorite branch contacts can minimize the total system energy by decreasing the total surfaces exposed. Such properties might help us to synthesize novel nanostructured designer materials.[25]

In conclusion, tree-like alumina nanopores were obtained in non-steady-state anodization conditions. This indicates that programming the non-steady-state anodization potential could help us to design more complex hierarchical pore architectures. As exemplified by gold nanotrees, the tree-like nanopores will be general templates towards fabrication of nanotrees from a variety of materials which are expected to exhibit novel shape-dependent properties.

Acknowledgements

Wenlong Cheng is grateful to the Alexander von Humboldt Foundation for financial support, and we thank also Kornelia Sklarek, Petra Göring, and Silko Grimm for technical support.

Notes and references

1 F. Keller, M. S. Hunter and D. L. Robinson, *J. Electrochem. Soc.*, 1953, **100**, 411.
2 J. P. O'Sullivan and G. C. Wood, *Proc. R. Soc. London, Ser. A*, 1970, **317**, 511.
3 G. E. Thompson and G. C. Wood, *Nature*, 1981, **290**, 230.
4 V. P. Parkhutik and V. I. Shershulsky, *J. Phys. D: Appl. Phys.*, 1992, **25**, 1258.
5 H. Masuda and K. Fukuda, *Science*, 1995, **268**, 1466.
6 S. Ono, M. Saito, M. Ishiguro and H. Asoh, *J. Electrochem. Soc.*, 2004, **151**, B473.
7 S. Z. Chu, K. Wada, S. Inoue, M. Isogai and A. Yasumori, *Adv. Mater.*, 2005, **17**, 2115.
8 W. Lee, R. Ji, U. Gosele and K. Nielsch, *Nat. Mater.*, 2006, **5**, 741.
9 S. Ono, M. Saito and H. Asoh, *Electrochem. Solid-State Lett.*, 2004, **7**, B21.
10 H. Masuda, H. Yamada, M. Satoh, H. Asoh, M. Nakao and T. Tamamura, *Appl. Phys. Lett.*, 1997, **71**, 2770.
11 R. B. Wehrspohn and J. Schilling, *MRS Bull.*, 2001, **26**, 623.
12 O. Jessensky, F. Muller and U. Gosele, *Appl. Phys. Lett.*, 1998, **72**, 1173.
13 G. Bahder, C. Katz, J. Lawson and W. Vahlstro, *IEEE Trans. Power Appar. Syst.*, 1974, **Pa93**, 977.
14 A. L. Barclay, P. J. Sweeney, L. A. Dissado and G. C. Stevens, *J. Phys. D: Appl. Phys.*, 1990, **23**, 1536.
15 R. M. Vadjikar, *J. Mater. Sci.*, 2004, **39**, 3487.
16 R. Hanaoka, S. Takata and Y. Nakagami, *IEEE Trans. Dielectr. Electr. Insul.*, 2004, **11**, 939.
17 M. A. El-Sayed, *Acc. Chem. Res.*, 2004, **37**, 326.
18 M. A. El-Sayed, *Acc. Chem. Res.*, 2001, **34**, 257.
19 G. E. Thompson, R. C. Furneaux, G. C. Wood, J. A. Richardson and J. S. Goode, *Nature*, 1978, **272**, 433.
20 J. Li, C. Papadopoulos and J. Xu, *Nature*, 1999, **402**, 253.
21 G. W. Meng, Y. J. Jung, A. Y. Cao, R. Vajtai and P. M. Ajayan, *Proc. Natl. Acad. Sci. U. S. A.*, 2005, **102**, 7074.
22 C. R. Martin, *Science*, 1994, **266**, 1961.
23 C. R. Martin, *Acc. Chem. Res.*, 1995, **28**, 61.
24 J. G. Wang, M. L. Tian, N. Kumar and T. E. Mallouk, *Nano Lett.*, 2005, **5**, 1247.
25 S. Park, J. H. Lim, S. W. Chung and C. A. Mirkin, *Science*, 2004, **303**, 348.
26 D. J. Pena, J. K. N. Mbindyo, A. J. Carado, T. E. Mallouk, C. D. Keating, B. Razavi and T. S. Mayer, *J. Phys. Chem. B*, 2002, **106**, 7458.
27 R. Koppe, G. Schmid, S. Schneider and H. Schnockel, *Eur. J. Inorg. Chem.*, 2005, 3657.
28 L. J. Zhi, J. S. Wu, J. X. Li, U. Kolb and K. Mullen, *Angew. Chem., Int. Ed.*, 2005, **44**, 2120.
29 M. Steinhart, J. H. Wendorff, A. Greiner, R. B. Wehrspohn, K. Nielsch, J. Schilling, J. Choi and U. Gosele, *Science*, 2002, **296**, 1997.
30 S. F. Hou, J. H. Wang and C. R. Martin, *Nano Lett.*, 2005, **5**, 231.